6-3Benchmarking Charge Trapping Models with NBTI, TDDS and RTN Experiments

Sharang Bhagdikar and Souvik Mahapatra*
Department of Electrical Engineering
Indian Institute of Technology Bombay
Mumbai 400076, India
*Phone: +91-222-572-0408, Email: souvik@ee.iitb.ac.in

***Abstract*-- A systematic review and comparison of existing charge trapping models in literature is performed. A framework for simulating hole trapping/de-trapping kinetics is established to compute resultant threshold voltage degradation (ΔV_{HT}) and capture-emission time constants ($\tau_C - \tau_E$). The models are analyzed by using data from Negative Bias Temperature Instability (NBTI), Random Telegraph Noise (RTN) and Time Dependent Defect Spectroscopy (TDDS) experiments.**

***Keywords*—NBTI, RTN, TDDS.**

I. INTRODUCTION

Charge trapping and detrapping in MOS dielectric contributes to NBTI, RTN, stress-induced leakage currents (SILC) and time dependent dielectric breakdown (TDDB) [1]-[5]. It is established that charge (hole in pFETs) trapping constitutes the overall threshold voltage (ΔV_{th}) degradation along with the interface trap (ΔV_{it}) and bulk trap (ΔV_{ot}) generation. Although numerous models have been proposed in an attempt at modelling the charge trapping time kinetics, the exact physical mechanism governing the process stays uncertain [6][7]. The four-state Extended Nonradiative Multiphonon Model (eNMP) [8] is touted to provide the most complete description of hole trapping kinetics. Capture and emission time constants of individual defects are modelled using eNMP [2]. However, the large number of tuning parameters make eNMP intractable and limit its practical use. The Two Well Nonradiative Multiphonon Model (2WNMP) is an abstraction of the eNMP model that treats the neutral and charged states of a trap as two energy levels represented as intersecting parabolic potential wells [8]. The macroscopic implementation of 2WNMP is used to model hole trapping in pre-existing defects in large area devices [7][9], and the stochastic implementation is used for NBTI and TDDS kinetics in small area devices [10]. The double well thermionic (DWT) model represents the distinct defect states as energy levels separated by a thermionic barrier. The original model [11] is altered in [12] by introducing a temperature activated barrier for modelling BTI kinetics over a range of temperatures. This Activated Barrier Double Well Thermionic (ABDWT) model [12] is invoked to model NBTI stress-recovery transients over a range of biases and temperatures and across different technologies [13]. The bias and temperature couplings of capture (τ_C) and emission (τ_E) time constants measured from TDDS and RTN studies is modelled using ABDWT [14].

II. MODEL FRAMEWORK & SIMULATION SETUP

Fig.1 depicts a schematic of the NMP model. The neutral (E_1) and charged (E_2) defect energy levels are approximated as quadratic potential wells. Level E_2 is pinned to the energy of the reservoir which supplies the carriers i.e. either the substrate conduction band edge (for electrons) or the valence band edge (for holes). The point where the wells intersect provide the barrier heights ϵ_{12} and ϵ_{21} for hole capture (k_{12}) and emission (k_{21}) rates respectively. The bias dependence gets accounted in the fact that upon application of a gate voltage, level E_1 undergoes an electrostatic level shift relative to E_2 (substrate) which would revise the barrier heights and, hence, the reaction rates. The required energy for the transition is supplied/dissipated entirely via phonons. The expressions for the reaction rates are rigorously derived in [8] and are listed in Fig.1.

The ABDWT model provides transition rates for charge (hole in p-FET) capture and emission within a trap, Fig.2. A transition from a reference neutral state (E_1) to the charged state (E_2) via a thermally activated barrier (E_B) constitutes the hole capture reaction. A backward transition signals the hole emission reaction. The barrier E_B and state E_2 lowers when a gate bias (V_G) is applied to account for the bias dependence on the reaction rates [13]. The parameters for bias-dependent barrier lowering and thermal lowering are distinct and allows for decoupling of bias and T dependence on rate constants.

Defects are distributed uniformly spatially in the dielectric for performing macroscopic simulations using 2WNMP. Appropriate model parameters (mean + spread) are assigned to be consistent with experimental data. Only the defects (E_1) that transition above or below the Fermi level upon application of bias may take part in the capture-emission reaction and are otherwise assumed to remain in equilibrium . The setup for the ABDWT model is similar except that the defects are situated at the dielectric-substrate interface owing to the fact that spatial dependence is implicitly captured by its parameters. For replication of defect-centric data (RTN, TDDS), an individual defect is placed in the dielectric and assigned unique model parameters to generate k_{12} and k_{21}, which yield τ_C and τ_E respectively.

III. NBTI MODELLING

Fig.3-4 shows experimental ΔV_{HT} stress and recovery data from Gate First HKMG planar MOSFETs [15]. The hole trapping component ΔV_{HT} is isolated from the measured mean ΔV_{TH} data using the macroscopic BAT framework [1], which uses an empirical relation to compute ΔV_{HT}. The ΔV_{HT} is thus extracted over a range of temperatures and biases using the

BAT framework. The ABDWT model simulations are shown to map the T activation over the entire range (Fig.5). ABDWT is shown to accurately model ΔV_{HT} stress data over a range of V_{GSTR} (Fig.6). Appropriate parameters for 2WNMP are selected to reproduce the stress data over the entire temperature range in Fig.7. It is observed that when the same parameters are used to model ΔV_{HT} stress data over a range of V_{GSTR}, 2WNMP predicts a stronger bias (V_{GSTR}) activation and the dataset cannot be matched (Fig.8). In Fig.9, suitable 2WNMP parameters are chosen to model the bias activation. The same parameters predict a weaker T activation and cannot map the entire T dataset (Fig.10). Similar analysis is carried out for ΔV_{HT} extracted from RMG HKMG SOI FinFETs [16]. ABDWT is shown to model ΔV_{HT} data in Figs.11-12 whereas simultaneous realization of bias and T activation cannot be achieved using 2WNMP, Figs.13-14. Comparison of ΔV_{HT} recovery curves over different V_{GREC} (Figs.15-16) and different stress times (Figs.17-18) is performed. It is observed that, for concurrent stress curves, the 2WNMP model predicts consistently slower recovery than ABDWT.

IV. RTN AND TDDS VALIDATION

Fig.19(a)-(d) list the distinct types of bias couplings (types A-D) for capture and emission time constants obtained from RTN studies [17]. All the different V_G couplings can be reproduced by the ABDWT model upon selection of suitable parameters. The type-A and type-B bias couplings are reproduced by 2WNMP. The presence of a bias-dependent pre-factor (p) in the 2WNMP capture rate expression prevents τ_C from being bias agnostic. In Fig.19(c), 2WNMP predicts a weak negative coupling of τ_C as opposed to the zero coupling observed. A negative coupling of τ_E, as observed in Fig.19(d), is realized in the *weak* electron-phonon coupling regime [8] of 2WNMP. τ_C in this regime is also negatively coupled with bias and it is not possible to achieve type-D coupling using 2WNMP. The dependence of τ_C and τ_E on V_G at different temperatures is recorded from RTN experiments in [18] and reproduced in Fig. 20. In Fig.21, ABDWT is shown to capture similar temperature activation trends across all V_G, owing to the fact that the τ_C and τ_E are not strongly coupled and can be tuned independently unlike in 2WNMP.

Fig.22 illustrates the bias dependence of τ_C and τ_E acquired from TDDS measurements for a non-switching trap [2]. The bias dependence is reproduced by ABDWT across two different T using appropriate parameters. The time constants for the non-switching trap are also modelled using 2WNMP. Figs.23-24 show TDDS time constants for switching trap with weak [2] and strong [19] bias activation of τ_E in the subthreshold region respectively. 2WNMP cannot replicate the switching behavior i.e. positive coupling of τ_E below threshold voltage.

V. CONCLUSION

Macroscopic frameworks of ABDWT and 2WNMP are used to model experimental NBTI data over a range of stress biases, recovery biases and temperatures. The 2WNMP model in its present form cannot predict T and V_{GSTR} activation as ABDWT, and is unable to model extended stress dataset. 2WNMP predicts slower ΔV_{HT} recovery than ABDWT. 2WNMP cannot reproduce the available capture and emission time constant bias couplings observed in RTN experiments. Switching trap time constants obtained using TDDS are not modelled by 2WNMP. τ_E and τ_C exhibit weaker correlation coming from ABDWT as compared to 2WNMP, which makes the former more versatile in modelling defect-centric data.

REFERENCES

[1] N. Parihar, N. Goel, S. Mukhopadhyay and S. Mahapatra, "BTI Analysis Tool-Modeling of NBTI DC, AC Stress and Recovery Time Kinetics, Nitrogen Impact, and EOL Estimation," in *IEEE Trans. Electron Devices*, vol. 65, no. 2, pp. 392-403, Feb.2018.

[2] T. Grasser, et al, "On the Microscopic Origin of the Frequency Dependence of Hole Trapping in pMOSFETs", *IEDM*, Dec. 2012, pp. 19.6.4.

[3] A. Kerber, A. Vayshenker, D. Lipp, T. Nigam and E. Cartier, "Impact of charge trapping on the voltage acceleration of TDDB in metal gate/high-k n-channel MOSFETs," 2010 *IEEE International Reliability Physics Symposium*, Anaheim, CA, 2010, pp. 369-372.

[4] W. Goes, M. Waltl, Y. Wimmer, G. Rzepa and T. Grasser, "Advanced modeling of charge trapping: RTN, 1/f noise, SILC, and BTI," 2014 *SISPAD*, Yokohama, 2014, pp. 77-80.

[5] N. Tega et al., "Increasing threshold voltage variation due to random telegraph noise in FETs as gate lengths scale to 20 nm," 2009 *Symposium on VLSI Technology*, Honolulu, HI, 2009, pp. 50-51.

[6] S. Mahapatra and Narendra Parihar, "A review of NBTI mechanisms and models," *Microelectron. Reliab*, Volume 81, 2018, Pages 127-135.

[7] Rzepa, G. et al. "Comphy - A compact-physics framework for unified modeling of BTI." *Microelectron. Reliab.* 85 (2018): 49-65.

[8] Grasser, T.. "Stochastic charge trapping in oxides: From random telegraph noise to bias temperature instabilities." *Microelectron. Reliab.* 52 (2012): 39-70.

[9] G. Rzepa et al., "Efficient physical defect model applied to PBTI in high-κ stacks," 2017 *IEEE International Reliability Physics Symposium (IRPS)*, Monterey, CA, 2017, pp. XT-11.1-XT-11.6.

[10] Anandkrishnan R, et al, "A Stochastic Modeling Framework for NBTI and TDDS in Small Area p-MOSFETs", *Simulation of Semiconductor Processes and Devices (SISPAD)* , Austin TX, Sep. 2018, pp. 181.

[11] D. Ielmini, et al, "A unified model for permanent and recoverable NBTI based on hole trapping and structure relaxation," *2009 IEEE International Reliability Physics Symposium*, Montreal, QC, 2009, pp. 26-32.

[12] S. Desai, et al, "A comprehensive AC / DC NBTI model: Stress, recovery, frequency, duty cycle and process dependence," *2013 IEEE International Reliability Physics Symposium (IRPS)*, Anaheim, CA, 2013, pp. XT.2.1-XT.2.11.

[13] N. Choudhury, N. Parihar, N. Goel, A. Thirunavukkarasu and S. Mahapatra, "A Model for Hole Trapping-Detrapping Kinetics During NBTI in p-Channel FETs: (Invited paper)," 2020 *4th IEEE Electron Devices Technology & Manufacturing Conference (EDTM)*, Penang, Malaysia, 2020, pp. 1-4.

[14] S. Bhagdikar and S. Mahapatra, "A Stochastic Hole Trapping-Detrapping Framework for NBTI, TDDS and RTN," *SISPAD*, Udine, Italy, 2019, pp. 1-4.

[15] N. Parihar, R. Anandkrishnan, A. Chaudhary and S. Mahapatra, "A Comparative Analysis of NBTI Variability and TDDS in GF HKMG Planar p-MOSFETs and RMG HKMG p-FinFETs," in *IEEE Transactions on Electron Devices*, vol. 66, no. 8, pp. 3273-3278, Aug. 2019.

[16] N. Parihar, U. Sharma, R. G. Southwick, M. Wang, J. H. Stathis and S. Mahapatra, "Ultrafast Measurements and Physical Modeling of NBTI Stress and Recovery in RMG FinFETs Under Diverse DC–AC Experimental Conditions," in *IEEE Transactions on Electron Devices*, vol. 65, no. 1, pp. 23-30, Jan. 2018.

[17] H. Miki, et al, "Understanding short-term BTI behavior through comprehensive observation of gate-voltage dependence of RTN in highly scaled high-κ / metal-gate pFETs", *Symposium on VLSI Technology - Digest of Technical Papers*, June 2011, pp. 149.

[18] H. Miki, et al, "Voltage and temperature dependence of random telegraph noise in highly scaled HKMG ETSOI nFETs and its impact on logic delay uncertainty", in *Symposium on VLSI Technology (VLSIT)*, pp. 138, June 2012.

[19] T. Grasser et al., "Advanced characterization of oxide traps: The dynamic time-dependent defect spectroscopy," 2013 *IEEE International Reliability Physics Symposium (IRPS)*, Anaheim, CA, 2013, pp. 2D.2.1-2D.2.7.

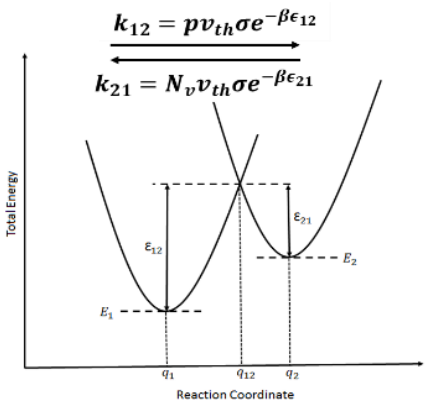

Fig.1. Schematic of 2WNMP model depicting potential wells of the neutral (q_1) and charged (q_2) states.

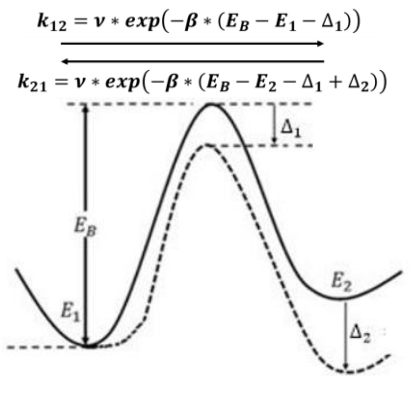

Fig.2. Schematic of ABDWT model. E_1, E_2 and E_b determine the energetic configuration of the trap.

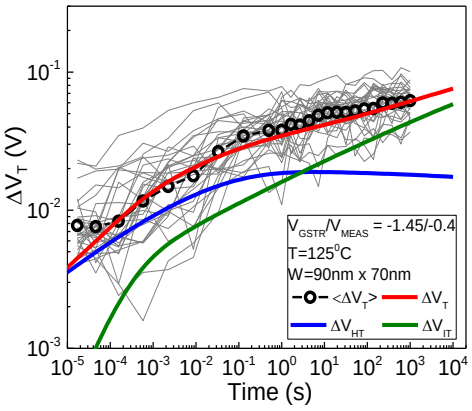

Fig.3. Individual (gray) and mean (black) measured ΔV_T traces during stress along with model calculated mean (red) and decomposition into subcomponents. Device is GF HKMG planar MOSFET.

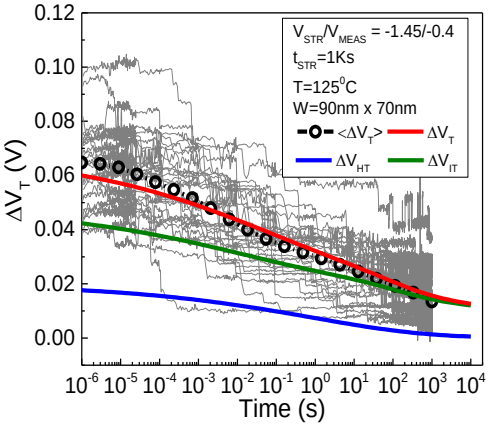

Fig.4. Individual (gray) and mean (black) measured ΔV_T traces during recovery along with model calculated mean (red) and decomposition into subcomponents

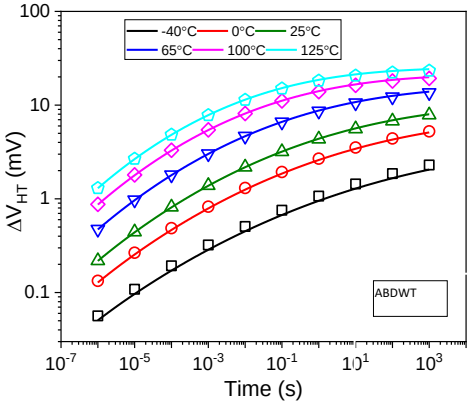

Fig.5. Modelling of ΔV_{HT} stress data (symbols) using ABDWT (solid lines) over a range of temperatures. GF HKMG planar MOSFETs

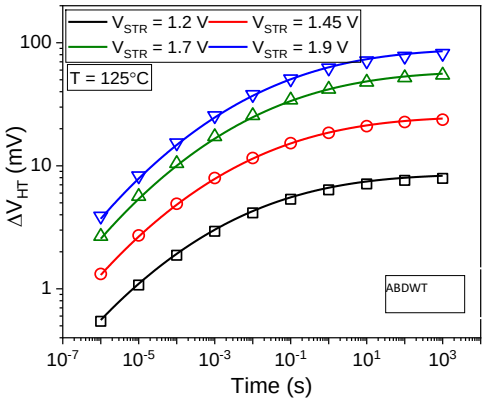

Fig.6. Modelling of ΔV_{HT} stress data (symbols) using ABDWT (solid lines) for a range of stress biases.

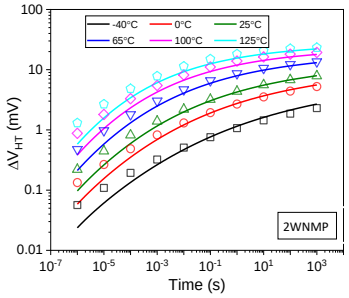

Fig.7. Modelling of ΔV_{HT} stress data (symbols) using 2WNMP (solid lines) over a range of temperatures.

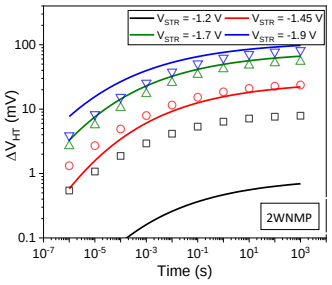

Fig.8. Modelling of ΔV_{HT} stress data using 2WNMP parameters of Fig.7. 2WNMP predicts stronger bias activation.

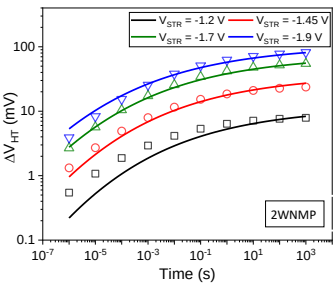

Fig.9. Modelling of ΔV_{HT} stress data (symbols) using 2WNMP (solid lines) for a range of biases.

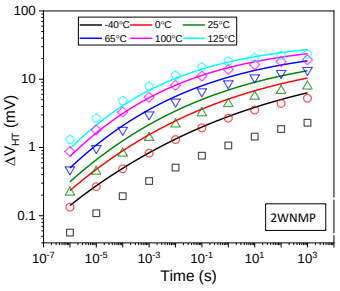

Fig.10. Modelling of ΔV_{HT} stress data using 2WNMP parameters of Fig.9. 2WNMP predicts weaker T activation.

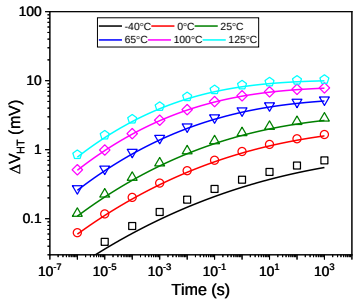

Fig.11. Modelling of ΔV_{HT} stress data (symbols) using ABDWT (solid lines) over a range of temperatures. Measurements are from RMG HKMG SOI FinFET.

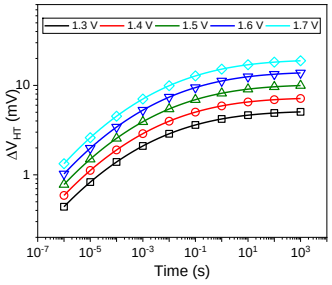

Fig.12. Modelling of ΔV_{HT} stress data (symbols) using ABDWT (solid lines) over a range of stress biases.

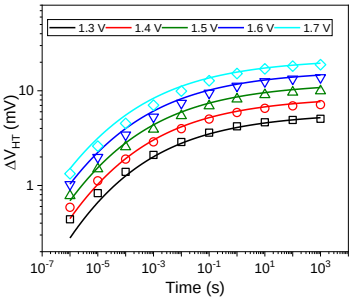

Fig.13. Modelling of ΔV_{HT} stress data (symbols) using 2WNMP (solid lines) for a range of biases.

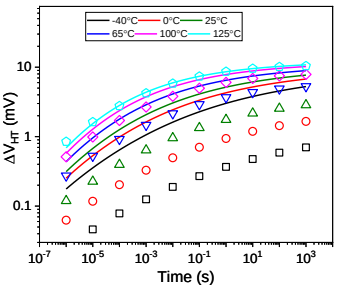

Fig.14. Modelling of ΔV_{HT} stress data using 2WNMP parameters used in Fig.13. 2WNMP predicts much weaker T activation.

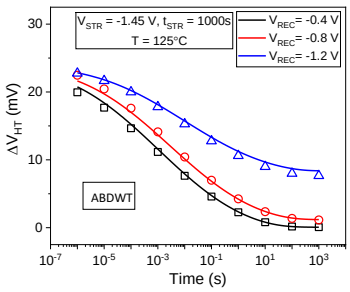

Fig.15. Modelling of ΔV_{HT} recovery data (symbols) using ABDWT (solid lines) for a range of recovery biases..

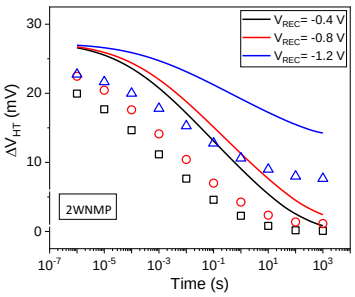

Fig.16. Modelling of ΔV_{HT} recovery data (symbols) using 2WNMP (solid lines) for a range of recovery biases.

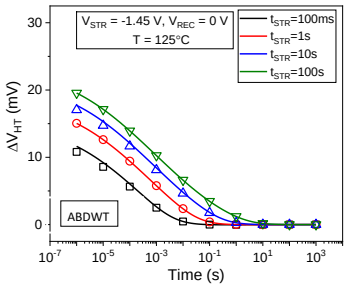

Fig.17. Modelling of ΔV_{HT} recovery data (symbols) using ABDWT (solid lines) for a range of stress times.

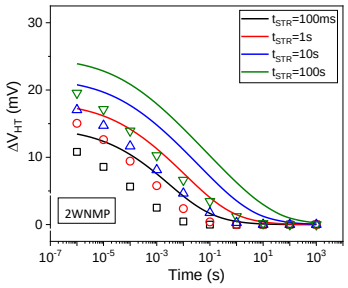

Fig.18. Modelling of ΔV_{HT} recovery data (symbols) using 2WNMP (solid lines) for a range of recovery biases.

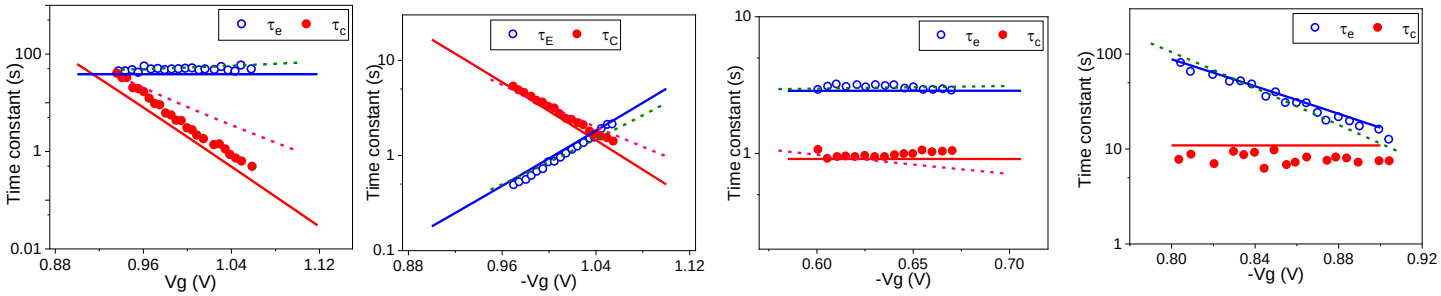

Fig.19(a)-(d). Panels depict various couplings of time constants to V_G extracted from RTN data (symbols) [12]. (A) $\tau_c < 0$, $\tau_e \sim 0$, (B) $\tau_c < 0$, $\tau_e > 0$, (C) $\tau_c \sim 0$, $\tau_e \sim 0$, (D) $\tau_c \sim 0$, $\tau_e < 0$. All the different couplings are reproduced using ABDWT model simulations (solid lines). 2WNMP simulations (dashed lines) can model type A and type B coupling upon selection of appropriate parameters. Zero coupling of τ_c with bias cannot be reproduced using 2WNMP and a negative coupling is observed in (c) and in (d) where τ_c is not shown (out of bounds, $\tau_C \gg \tau_E$).

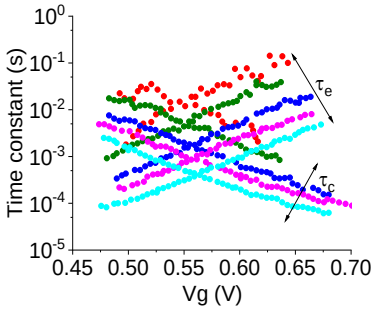

Fig.20. Time constants as a function of V_G at various temperatures from RTN experiments [18].

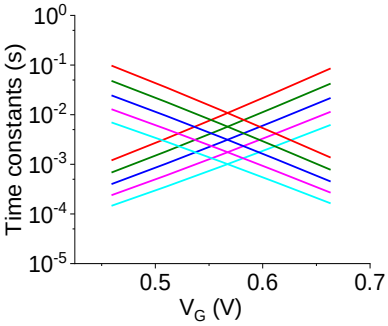

Fig.21. ABDWT model simulated time constants as a function of V_G at various temperatures.

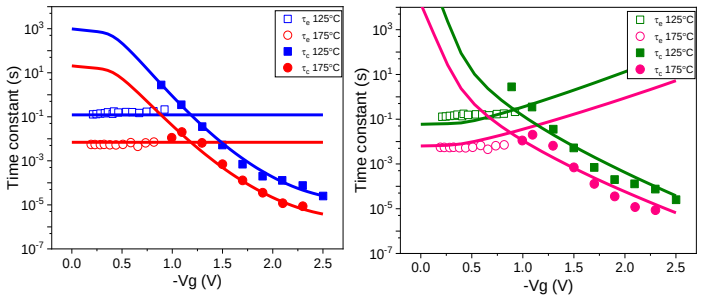

Fig.21. Modelling of TDDS capture and emission time constants (symbols) for non-switching trap [2] using ABDWT (left) and 2WNMP (right). Non-switching nature is evident by the bias agnostic τ_E in the subthreshold regime.

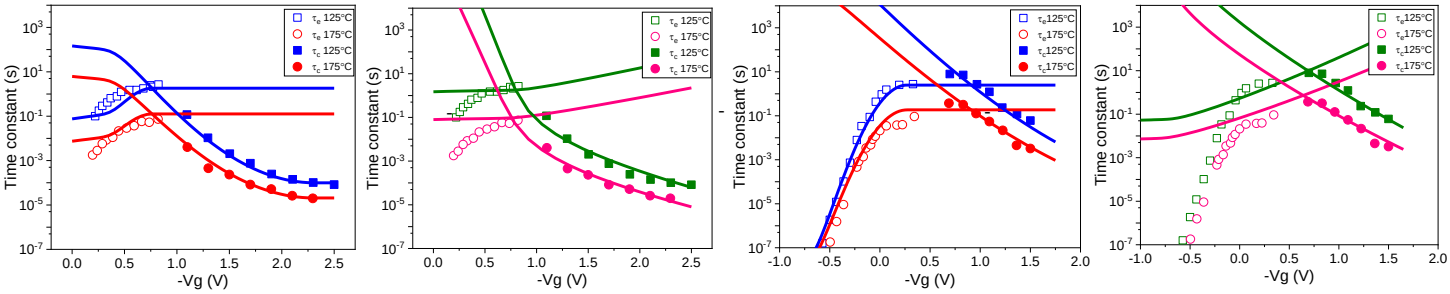

Fig.22. Modelling of TDDS capture and emission time constants (symbols) for non-switching trap [2] using ABDWT (left) and 2WNMP (right). Switching behavior is evident by the positive bias coupling of τ_e with V_G.2WNMP in its present form is unable to replicate said coupling.

Fig.23. Modelling of TDDS capture and emission time constants (symbols) for switching trap B3 [19] using ABDWT (left) and 2WNMP (right).